Noise-induced escape of periodically modulated systems: From weak to strong modulation

D. Ryvkine and M. I. Dykman
Department of Physics and Astronomy, Michigan State University, East Lansing, Michigan 48824, USA
(Received 14 April 2005; published 25 July 2005)

Noise-induced escape from a metastable state is studied for an overdamped periodically modulated system. We develop an asymptotic technique that gives both the instantaneous and period-average escape rates, including the prefactor, for an arbitrary modulation amplitude A. We find the parameter range where escape is strongly synchronized and the instantaneous escape rate displays sharp peaks. The peaks vary with increasing modulation frequency or amplitude from Gaussian to strongly asymmetric. The prefactor ν in the period-average escape rate depends on A nonmonotonically. Near the bifurcation amplitude A_c it scales as $\nu \propto (A_c - A)^{\zeta}$. We identify three scaling regimes, with $\zeta = 1/4$, -1, and $1/2$.

DOI: 10.1103/PhysRevE.72.011110 PACS number(s): 05.40.−a, 02.50.−r, 05.70.Ln, 77.80.Fm

I. INTRODUCTION

Noise-induced escape from a metastable state is an interesting effect of the interplay of nonlinear dynamics and fluctuations that has been attracting much attention since the Kramers paper [1]. Escape and the resulting interstate switching are becoming increasingly more important for applications, particularly in nanotechnology where the size of the system is small and fluctuations are comparatively large. Recently much work on escape has been done for systems driven by time-dependent fields. Examples include transitions in modulated nano- and micromechanical oscillators [2,3], Josephson junctions [4–6], and nanomagnets [7–9]. Modulation changes the activation barrier. This enables both efficient control of the escape rate and accurate measurement of the system parameters [2,10]. Because in escape the system moves far away from its metastable states, studying escape provides an insight into the global dynamics of the system.

The most frequently used types of modulation are ramping of a control parameter and periodic modulation. Ramping is usually done slowly, and it is assumed that the system remains quasistationary [11]. Periodic modulation is conceptually simpler as periodic metastable states are well defined irrespective of the modulation frequency. However, a theory of the escape rate is more complicated, because the system is away from thermal equilibrium [12]. Recently significant attention was attracted also to escape over a randomly fluctuating barrier [13,14].

In the present paper we study periodically modulated systems and extend to them the analysis of the escape rate done by Kramers for systems in thermal equilibrium [1]. Our approach gives the full time-dependent escape rate $W(t)$ as well as the period-average rate $\bar{W} = \nu \exp(-R/D)$, where R is the activation energy of escape and D is the noise intensity, $D = k_B T$ for thermal noise. We find $W(t)$ for an arbitrary modulation amplitude A and an arbitrary interrelation between the modulation frequency ω_F and the relaxation time of the system t_r. We show that the prefactor ν depends on A strongly and nonmonotonically. It displays scaling behavior near the bifurcational modulation amplitude A_c where the metastable state of the system disappears. Preliminary results of this work were reported earlier [15].

In the absence of modulation escape can happen at any time with the same probability density. For systems in thermal equilibrium, the activation energy equals the free energy barrier height. The prefactor ν is given by the generalized attempt frequency and does not depend on D for not too small damping [1].

Even a comparatively weak driving can exponentially strongly modulate the escape rate leading to strong escape synchronization for small D [16]. This is easy to see for a Brownian particle in a slowly modulated potential well [see Fig. 1(a)]: it is most likely to escape once per modulation period when the barrier is at its lowest. The "time window" for escape is diffusion broadened. Therefore the period-average escape rate is $\bar{W} \propto D^{1/2}$ [17].

For an overdamped Brownian particle a transition, with increasing modulation amplitude A, from the D-independent prefactor in the absence of modulation [1] to $\nu \propto D^{1/2}$ was discussed in Ref. [17]. However, the results were limited to comparatively weak modulation, region I in Fig. 1(b). The

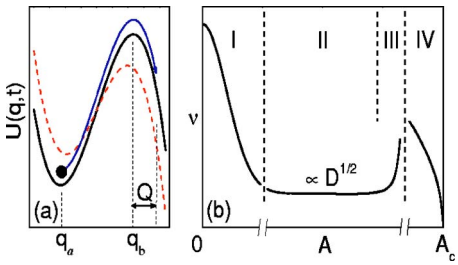

FIG. 1. (Color online) (a) An oscillating potential barrier. In the limit of slow modulation, the stable and unstable periodic states q_a and q_b are the instantaneous positions of the potential minimum and barrier top, respectively. The instantaneous escape rate is characterized by the current at an "observation point" located at a sufficiently large distance Q from q_b. (b) The dependence of the prefactor ν in the period-average escape rate $\bar{W} = \nu \exp(-R/D)$ on the modulation amplitude A (schematically). For $A \to 0$, ν is given by the Kramers theory [1]. In regions II and III escape is synchronized and $\nu \propto D^{1/2}$, where D is the noise intensity. In region III, close to the critical point A_c where the metastable state disappears, the prefactor scales as $\nu \propto (A_c - A)^{-1}$. In region IV $\nu \propto (A_c - A)^{1/2}$ is independent of D.

range of intermediate modulation, region II, was discussed in Refs. [18,19]. However, the obtained prefactor in the period-average rate diverges for $A \to 0$. The approach of Ref. [18] is inapplicable for slow modulation compared to the relaxation time of the system. In contrast, the technique developed in the present paper is free from these limitations. The scaling regions III and IV and the strongly nonmonotonic behavior of the prefactor have not been previously identified.

To find the instantaneous escape rate $W(t)$ we relate it, in the spirit of Kramers' approach, to the current *well behind* the boundary $q_b(t)$ of the basin of attraction to the initially occupied metastable state (q is the system coordinate). We call the current away from the attraction basin the escape current. In stationary systems and for the time $t \ll W^{-1}$ the escape current is independent of the coordinate and is the same on the basin boundary and behind it. In periodically modulated systems this is no longer the case. A particle that crossed the boundary at one time may cross it back at a later time, because the boundary itself is moving. In experiments the position of the instantaneous basin boundary is not necessarily known. The current is usually detected well behind the boundary, for example, close to another metastable state. The functional form of this current is qualitatively different from that at $q_b(t)$ calculated in Refs. [18,19].

The escape current can be obtained by relating the probability distributions of the system $\rho(q,t)$ behind the boundary $q_b(t)$ and close to the attractor $q_a(t)$ from which the system escapes. We do this in two steps. First, we find the general form of the current-carrying distribution $\rho(q,t)$ in the boundary layer about $q_b(t)$, where the equation of motion of the system can be linearized. Then we match it to the distribution inside the attraction basin but well outside the diffusion layer around $q_b(t)$. This distribution can be obtained in the eikonal approximation for small D. It has singular features [20]. The matching is performed using these singular features.

In Sec. II we describe the model and give the general form of the boundary-layer distribution. In Sec. III this distribution is used to obtain general expressions for the instantaneous and period-average escape rate. Matching of the intrawell and boundary-layer distributions is discussed in Sec. IV. In Sec. V we study the pulse shape of synchronized escape current in different regimes. Section VI provides a brief discussion of the period-average escape rate in the regions I and II in Fig. 1(b). In Sec. VII we identify three different types of the scaling behavior of the prefactor ν close to the bifurcation point and find the critical exponents. In Sec. VIII the general results are compared with Monte Carlo simulations for a specific system. In Sec. IX we summarize the results and sketch a surprisingly rich map of different types of escape behavior in the plane of modulation parameters.

II. THE MODEL AND THE BOUNDARY-LAYER DISTRIBUTION

Escape from a metastable state of a periodically modulated system is well characterized if the noise is weak, so that the escape rate $W \ll t_r^{-1}, \omega_F$. In this case, over the relaxation time t_r the periodically modulated system will most likely approach its periodic metastable state (attractor) with the coordinate $q_a(t)=q_a(t+\tau_F)$ ($\tau_F=2\pi/\omega_F$ is the modulation period). Then most likely, it will be performing small fluctuations about q_a and will "forget" the initial state $q(0)$. Eventually there will occur a large fluctuation in which the system will go over the boundary $q_b(t)$ and leave the basin of attraction, i.e., escape.

The instantaneous escape rate $W(t)$ is characterized by the current $\langle \dot{q}(t) \rangle$ away from the metastable state. The current has to be measured well behind the boundary $q_b(t)$, so that the system in practice does not return to the metastable state.

The probability distribution $\rho(q,t)$ of a periodically modulated overdamped Brownian particle is given by the Fokker-Planck equation (FPE)

$$\partial_t \rho = -\partial_q [K(q,t)\rho] + D\partial_q^2 \rho. \tag{1}$$

Here, $K(q,t)$ is the periodic force driving the particle, $K(q,t)=K(q,t+\tau_F) \equiv -\partial_q U(q,t)$, where $\tau_F=2\pi/\omega_F$ is the modulation period and $U(q,t)$ is the instantaneous potential.

The equation of motion of the particle in the absence of noise is $\dot{q}=K(q,t)$. The metastable state $q_a(t)$, from the vicinity of which the system escapes due to noise, and the basin boundary $q_b(t)$ are the stable and unstable periodic solutions of this equation, respectively.

We will assume that the noise intensity D is small. Then in a broad time range $t_r \ll t \ll 1/\bar{W}$ the distribution $\rho(q,t)$ is nearly periodic in the basin of attraction to $q_a(t)$. The current away from this basin and thus the escape rate $W(t)$ are also periodic.

A. Motion near periodic states

The distribution ρ is maximal at the metastable state $q_a(t)$ and falls off exponentially away from it. In the presence of periodic driving it acquires singular features as $D \to 0$ [20], some of which have counterparts in wave fields [21], with D playing the role of the wavelength. The singularities accumulate near $q_b(t)$. In order to find $W(t)$ one has to understand how they are smeared by diffusion.

In the absence of noise the motion of the system close to the periodic states $q_i(t)$ ($i=a,b$) is described by the equation $\dot{q}=K$ with K linearized in $\delta q=q-q_i(t)$:

$$\delta\dot{q} = \mu_i(t)\,\delta q, \quad \mu_i(t) = \mu_i(t+\tau_F) \equiv [\partial_q K]_{q_i(t)}. \tag{2}$$

The evolution of $\delta q(t)$ is given by $\delta q(t)=\kappa_i(t,t')\delta q(t')$, where

$$\kappa_i(t,t') = \exp\left[\int_{t'}^{t} d\tau\, \mu_i(\tau)\right] \quad (i=a,b). \tag{3}$$

Over the period τ_F the distance δq decreases (for $i=a$) or increases (for $i=b$) by the Floquet multiplier

$$M_i = \kappa_i(t+\tau_F,t) \equiv \exp(\bar{\mu}_i \tau_F),$$

where $\bar{\mu}_i$ is the period-average value of $\mu_i(t)$, with $\bar{\mu}_a<0$, $\bar{\mu}_b>0$.

For weak noise the linearized force K can be used to find $\rho(q,t)$ near $q_{a,b}(t)$. Near the metastable state q_a, the distribution ρ is Gaussian [22],

$$\rho(q,t) = \frac{1}{\sqrt{2\pi D\sigma_a^2(t)}} \exp\left\{-\frac{[q-q_a(t)]^2}{2D\sigma_a^2(t)}\right\}. \tag{4}$$

The time-periodic variance is

$$\sigma_i^2(t) = 2|M_i^{-2}-1|^{-1}\int_0^{\tau_F} dt_1 \kappa_i^{-2}(t+t_1,t) \tag{5}$$

with $i=a$; in the absence of modulation $\sigma_a^2 = 1/|\mu_a|$.

B. Distribution near the unstable state

The periodic distribution near the unstable state $q_b(t)$, i.e., the boundary-layer distribution, is substantially non-Gaussian. It corresponds to a periodic current away from the attraction basin. The distribution can be found from Eq. (1) using the Laplace transform, similar to the weak-driving limit [17]:

$$\rho(q,t) = \int_0^\infty dp\, e^{-pQ/D}\tilde{\rho}(p,t), \quad Q = q - q_b(t). \tag{6}$$

We assume that Q is small, $|Q| \ll \min_t|q_b(t)-q_a(t)|$. Using the expansion $K=\dot{q}_b(t)+\mu_b(t)Q$, we obtain from the FPE (1) a first-order equation for the Laplace transform $\tilde{\rho}(p,t)$

$$\partial_t\tilde{\rho} = \mu_b(t)p\partial_p\tilde{\rho} + (p^2/D)\tilde{\rho}. \tag{7}$$

This equation can be solved by the method of characteristics, giving

$$\tilde{\rho}(p,t) = \mathcal{E}D^{-1/2}\exp\{-[s(\phi) + p^2\sigma_b^2(t)/2]/D\}. \tag{8}$$

In Eq. (8), $\mathcal{E}$ is a constant and $s(\phi)$ is an arbitrary zero-mean periodic function, $s(\phi+2\pi)=s(\phi)$. They have to be found by matching $\rho(q,t)$ (6) to the distribution inside the attraction basin. The function $\sigma_b^2(t)$ in Eq. (8) is given by Eq. (5) with $i=b$, and the factor $D^{-1/2}$ is singled out for convenience.

The phase of the function s is $\phi \equiv \phi(p,t)$,

$$\phi(p,t) = \Omega_F \ln[p\kappa_b(t,t')/\bar{\mu}_b l_D]. \tag{9}$$

Here,

$$\Omega_F = \omega_F/\bar{\mu}_b \equiv 2\pi/\ln M_b$$

is the reduced field frequency, $l_D=(2D/\bar{\mu}_b)^{1/2}$ is the typical diffusion length, and t' determines the initial value of ϕ. From Eq. (9), $\phi(p,t+\tau_F)=\phi(p,t)+2\pi$.

III. INSTANTANEOUS AND PERIOD-AVERAGE ESCAPE RATE

A. General expression for the escape rate

The experimentally accessible instantaneous rate of escape from the metastable state is characterized by the current $j(q,t)$ from its attraction basin. We assume that this basin lies for $q<q_b(t)$, i.e., $q_a(t)<q_b(t)$. Then the escape current is the rate of change of the population in the region $(-\infty,q]$, with q lying behind the basin boundary $q_b(t)$. As explained in the Introduction, of interest is $j(q,t)$ for such q that $Q=q-q_b(t) \gg l_D$. Equation (6) is advantageous as it immediately gives such a current.

We consider first $j(q,t)$ not for a fixed q, but for a fixed distance $Q=q-q_b(t)$ from the boundary,

$$j(q,t) = -\frac{\partial}{\partial t}\int_{-\infty}^{q_b(t)+Q} dq\, \rho(q,t) \approx \mu_b(t)\rho(q_b(t)+Q,t)Q. \tag{10}$$

Here we have used the FPE (1) and linearized $K(q_b(t)+Q,t)$ in Q; we have also disregarded the diffusion current, which is a good approximation for $Q \gg l_D$.

The distribution $\rho(q_b(t)+Q,t)$ in the expression for the current (10) is given by Eqs. (6) and (8). For $Q \gg l_D$ the term proportional to p^2/D in Eq. (8) can be neglected compared to pQ/D. Changing in Eq. (6) to integration over $x=pQ/D$, we obtain

$$j(q,t) = \mu_b(t)\mathcal{E}D^{1/2}\int_0^\infty dx\, e^{-x}\exp[-s(\phi_d)/D],$$

$$\phi_d = \phi(xD/Q,t) = \Omega_F \ln[x\kappa_b(t_d,t')]. \tag{11}$$

Here $t_d \equiv t_d(Q,t)$ is given by the equation $\kappa_b(t_d,t)=l_D/2Q$.

It follows from Eq. (11) that in the whole harmonic region j depends on the observation point Q only in terms of the delay time t_d. This time shows how long it takes the system to roll down to the point Q, $\partial_Q t_d = -1/[\mu_b(t_d)Q]$. We note that $\mu_b(t)$ can be negative for a part of the period, leading to reversals of the instantaneous current.

The escape rate $\bar{W}$ is given by the period average $j(q,t)$. The averaging can be done for a given q or a given Q behind the boundary. The result will be the same, since the period-average value of $\partial_q j$ is equal to zero, and therefore the period-average current is independent of coordinate. It is convenient to do time averaging in Eq. (11) by changing from integration over time to integration over ϕ_d with account taken of the relation $d\phi_d/dt=\Omega_F\mu_b(t)$. The result is independent of Q, as expected, and reads

$$\bar{W} = \frac{\bar{\mu}_b}{2\pi}\mathcal{E}D^{1/2}\int_0^{2\pi} d\phi \exp[-s(\phi)/D]. \tag{12}$$

Equations (11) and (12) provide a complete solution of the Kramers problem of escape of a modulated system and reduce it to finding the function s. It is seen from Eqs. (8) and (12) that this function has the meaning of the zero-mean periodic part of the activation energy of escape. Equations (11) and (12) are similar in form to the expressions for the instantaneous and average escape rates for comparatively weak modulation obtained in Ref. [17]. For such modulation $|s| \ll R$, which allowed finding s explicitly (see Appendix A).

B. Synchronization of escape

Periodic modulation may lead to an exponentially strong time dependence of the escape probability within a period,

that is, to *synchronization* of escape events. This effect is determined by the parameter $|s_m|/D$. Here $s_m \equiv \min_\phi s(\phi)$ is the minimal value of s reached for a certain phase $\phi=\phi_m$. By construction, $s_m<0$. We will be interested in *strong* synchronization, when the escape current displays sharp narrow periodic peaks as a function of time.

Strong synchronization of escape requires that $|s_m| \gg D$ (a more precise criterion will be discussed below). In this case the factor $\exp[-s(\phi_d)/D]$ in Eq. (11) for $j(q,t)$ is a sharp function of ϕ_d. The major contribution to the integral over x comes from the range where s is close to s_m and, respectively, the phase ϕ_d is close to ϕ_m. The time dependence of $j(q,t)$ can be found by changing in Eq. (11) from integration over x to integration over ϕ_d. Because $|s_m| \gg D$, the integrand $(dx/d\phi_d)\exp[-x-(s/D)]$ is maximal for $\phi_d=\phi_m-2\pi k$ with $k=0,\pm 1,\ldots$. For such ϕ_d and for a given k the integrand is equal to

$$g_k(t) = \Omega_F^{-1} x_k \exp[-x_k - (s_m/D)],$$

where

$$x_k(t) = \kappa_b^{-1}(t_d,t')\exp[(\phi_m + 2\pi k)/\Omega_F]. \tag{13}$$

The whole integral (11) is determined by the sum of g_k.

As a function of time, g_k is maximal for $x_k=1$. Within any period of time from t to $t+\tau_F$ the condition $x_k=1$ is met only for one k, and only for one instant of time t_k. For all other k the function $x_k \exp(-x_k)$ is much smaller provided $\Omega_F \lesssim 1$. We note that, if $x_k=1$ for a given t_k, then it follows from Eqs. (3) and (13) that $x_{k+1}=1$ for $t_{k+1}=t_k+\tau_F$. This means that, as a function of time, the escape rate displays sharp periodic peaks with period τ_F. The shape of the peaks will be discussed below.

When $|s_m| \ll D$, there is no exponential synchronization, and the escape current smoothly depends on time. It happens in particular when modulation is weak or the modulation frequency is large, $\Omega_F \gg 1$.

IV. MATCHING THE INTRAWELL AND BOUNDARY-LAYER DISTRIBUTIONS

A. Intrawell distribution near the basin boundary

To find $j(q,t)$ we match the boundary-layer distribution (6) to the tail of the intrawell distribution. The matching has to be done close to the basin boundary $q_b(t)$, where Eq. (6) applies, but it is convenient to do it well inside the attraction basin, $-[q-q_b(t)] \gg l_D$, that is, outside the diffusion layer around $q_b(t)$. Of primary interest is the case of strong modulation, $|s_m| \gg D$, since the case of weak to moderately strong modulation was considered earlier [17].

The intrawell distribution in the region $-Q \gg l_D$ [$Q=q-q_b(t)$] can be found, for example, by solving the FPE (1) in the eikonal approximation, with the diffusion coefficient D being a small parameter,

$$\rho(q,t) = e^{-S(q,t)/D}, \quad S = S_0 + DS_1 + \cdots \tag{14}$$

(here, in contrast to Ref. [15] we single out the factor D in S_1 explicitly).

To zeroth order in D, the equation for $S_0 \equiv S_0(q,t)$ can be written as

$$\partial_t S_0 = -H(\partial_q S_0, q; t). \tag{15}$$

Equation (15) has the form of a Hamilton-Jacobi equation for the action S_0 of an auxiliary conservative system with Hamiltonian [23]

$$H(p,q;t) = p^2 + pK(q,t), \quad p = \partial_q S_0. \tag{16}$$

The auxiliary system is nonautonomous, its Hamiltonian is a periodic function of time. Since we are interested in the periodic distribution $\rho(q,t)$, we need to find a periodic solution of Eq. (15). This can be done using the method of characteristics, i.e., by studying Hamiltonian trajectories $(q(t),p(t))$ of the auxiliary system,

$$\dot{q} = K + 2p, \quad \dot{p} = -p\partial_q K. \tag{17}$$

Equations (17) have two hyperbolic periodic states $(q_a(t),0)$ and $(q_b(t),0)$, where $q_a(t)$ and $q_b(t)$ are the metastable state and the basin boundary of the original dissipative system. We are interested in Hamiltonian trajectories $(q(t),p(t))$ that belong to the *unstable* manifold of the periodic state $(q_a(t),0)$. For such trajectories, the action $S_0(q,t)$ is minimal for $q=q_a(t)$, and $\rho(q,t)$ is maximal, respectively. Indeed, a straightforward calculation based on Eq. (17) shows that, for q close to $q_a(t)$, the momentum on the unstable manifold is $p=[q-q_a(t)]/\sigma_a^2(t)$, where σ_a^2 is given by Eq. (5). Respectively, $S_0=[q-q_a(t)]^2/2\sigma_a^2(t)$, in agreement with Eqs. (4) and (14) for $\rho(q,t)$.

To logarithmic accuracy, the escape rate is determined by the probability to reach the basin boundary $q_b(t)$, i.e., by the action $S_0(q_b(t),t)$ [16]. The Hamiltonian trajectories of the auxiliary system that form this action belong to the *stable* manifold of the periodic state $(q_b(t),0)$. The trajectory $(q_{\rm opt}(t),p_{\rm opt}(t))$, which minimizes $S_0(q_b(t),t)$, approaches $q_b(t)$ asymptotically as $t\to\infty$. This is a heteroclinic trajectory of the auxiliary system, an intersection of the unstable and stable manifolds of the states $(q_a(t),0)$ and $(q_b(t),0)$, respectively [20].

In the case of dissipative systems with detailed balance, including systems in thermal equilibrium, the corresponding manifolds coincide with each other. However, in nonequilibrium systems this is no longer true. In periodically modulated systems there is only one heteroclinic trajectory with minimal S_0 per period. The coordinate $q_{\rm opt}(t)$ on this trajectory is the most probable escape path (MPEP). This is the trajectory that the original system is most likely to follow in escape. It is physically observable and has been seen in both experiments and simulations [16].

Close to $q_b(t)$, the Hamiltonian equations (17) for $q(t),p(t)$ can be linearized and solved. On the MPEP

$$p_{\rm opt}(t) = -Q_{\rm opt}(t)/\sigma_b^2(t) = \kappa_b^{-1}(t,t')p_{\rm opt}(t'),$$

$$S_0(q_{\rm opt}(t),t) = R - Q_{\rm opt}^2(t)/2\sigma_b^2(t), \tag{18}$$

where $Q_{\rm opt}(t)=q_{\rm opt}(t)-q_b(t)$. The quantity $R=S_0(q_{\rm opt}(t),t)_{t\to\infty}$ is the activation energy of escape.

Equations (18) apply to an arbitrary trajectory on the stable manifold of the state $(q_b(t),0)$ close to this state. The MPEP is just one such trajectory. It is determined by the condition that it starts at $(q_a(t),0)$ for $t\to-\infty$. This condition synchronizes the trajectory and determines $p_{\rm opt}(t)$ for a given t. It is important that the optimal paths are periodically repeated in time with period τ_F. The values of $p_{\rm opt}(t)$ form an infinite series. For neighboring paths they differ by the factor M_b^{-1}. They can also be thought of as the values of $p_{\rm opt}(t+k\tau_F)$ for the same MPEP and different k, with $p_{\rm opt}(t+k\tau_F)\to 0$ for $k\to\infty$.

From Eqs. (18), everywhere on the stable manifold of $(q_b(t),0)$ the action has the form

$$S_b(q,t) = R - Q^2/2\sigma_b^2(t). \tag{19}$$

It is parabolic as a function of Q.

Due to nonintegrability of the dynamics with Hamiltonian (16), the action surface $S_0(q,t)$, which gives the intrawell probability distribution (14), becomes flat for small $Q-Q_{\rm opt}$ [20]. It touches the surface $S_b(q,t)$ on the MPEP. Away from the MPEP $S_0(q,t)>S_b(q,t)$. Therefore the function

$$\rho_b(q,t) = \rho(q,t)\exp[S_b(q,t)/D] \tag{20}$$

is maximal on the MPEP.

The prefactor of the eikonal-approximation distribution is given by the term $\exp(-S_1)$; cf. Eq. (14). On the MPEP the auxiliary function $z=\exp(2S_1)$ obeys the equation [24]

$$\frac{d^2z}{dt^2} - 2\frac{d(z\partial_q K)}{dt} + 2zp\partial_q^2 K = 0, \tag{21}$$

where $q=q_{\rm opt}(t)$, $p=p_{\rm opt}(t)$. The initial condition to this equation follows from the explicit form (4) of $\rho(q,t)$ near the stable state,

$$z(t) \to 2\pi D\sigma_a^2(t), \quad t\to-\infty. \tag{22}$$

Close to $q_b(t)$, from Eq. (21),

$$z(t) = D[\mathcal{Z}_1\sigma_b^2(t) + \mathcal{Z}_2 p_{\rm opt}^{-2}(t)], \tag{23}$$

where $\mathcal{Z}_{1,2}$ are constants [18,25]. This solution was found in Ref. [18], but the term proportional to $\mathcal{Z}_1$ was disregarded.

B. Matching the exponents and prefactors

We are now in a position to match the functions $\rho_b(q,t)$ [Eq. (20)] as given by the eikonal approximation (14), (18), and (23) and the boundary-layer solution (6). In the spirit of the eikonal approximation, matching should be done in the vicinity of the MPEP, where ρ_b is maximal.

The eikonal approximation applies when the optimal escape paths $q_{\rm opt}(t+k\tau_F)$ $(k=0,\pm1,\dots)$ are separated by a large distance compared to the diffusion length l_D. For small noise intensity D the corresponding range incorporates much of the harmonic region near $q_b(t)$, because the width of the latter region Δq is independent of D and $\Delta q \gg l_D$ for small D. Physically, l_D characterizes the width of the tube of paths along which the system moves in escape [16]. In the region $-Q\lesssim l_D$ the tubes of escape paths overlap and the eikonal approximation no longer applies.

In contrast, the boundary-layer distribution Eq. (6) covers the whole harmonic region $|Q|\ll\Delta q$, including the diffusion-dominated region $|Q|\lesssim l_D$. Thus, for small noise intensity D, the two distributions should overlap in a broad range $l_D\ll -Q\ll\Delta q$ inside the harmonic region but outside the diffusion-dominated layer.

We first consider the boundary-layer expression (6) for $\rho_b(q,t)$ in the region $-Q\gg l_D$ and for strong modulation $|s_m|\gg D$. As we show, $\rho_b(q,t)$ is maximal for all times t provided q lies on an appropriate trajectory that belongs to the stable manifold of $q_b(t)$.

Equation (6) is simplified for $-Q\gg l_D$, because the integral over p can be evaluated by the steepest descent method. The extremum of the integrand is given by the condition

$$p\sigma_b^2(t) + Q + \Omega_F p^{-1}\frac{ds}{d\phi} = 0.$$

The integrand is maximal if $p=-Q/\sigma_b^2(t)$ and s is minimal for this p, i.e., $\phi(p,t)=\phi_m$ and $s=s_m$. The relation $p=-Q/\sigma_b^2(t)$ holds for any trajectory on the stable manifold of $q_b(t)$; cf. Eq. (18). Moreover, since on these trajectories $p=p(t)=\kappa_b^{-1}(t,t')p(t')$, it follows from Eq. (9) that $\phi(p,t)=$const. Therefore if the phase $\phi=\phi_m$ for one instant of time, it will be equal to ϕ_m for all times.

The function ρ_b (20) calculated in the eikonal approximation is maximal on the MPEP. Therefore ρ_b in the boundary-layer approximation should be maximal on the MPEP as well. It follows from the above arguments that it will indeed be maximal on the MPEP provided

$$\phi(p_{\rm opt}(t),t) = \phi_m. \tag{24}$$

This amounts to choosing the appropriate initial phase (the value of t') in Eq. (9). With this choice, steepest descent integration in Eq. (6) gives the boundary-layer distribution near the MPEP in the form

$$\rho(q,t) = \mathcal{E}_b(t)\exp[-S_b(q,t)/D],$$

$$\mathcal{E}_b(t) = \widetilde{\mathcal{E}}D^{-1/2}[\sigma_b^2(t) + \Omega_F^2 s_m'' p_{\rm opt}^{-2}(t)]^{-1/2}, \tag{25}$$

where

$$\widetilde{\mathcal{E}} = \mathcal{E}(2\pi D)^{1/2}\exp[(R-s_m)/D],$$

$$s_m'' = [d^2s/d\phi^2]_{\phi_m}. \tag{26}$$

It is seen from Eqs. (18) and (25) that, with the right choice of phase, the exponents of the boundary-layer and eikonal-approximation distributions coincide with each other along the MPEP. Moreover, the slopes $\partial_q S_b(q,t)$, which are determined by $p_{\rm opt}(t)$, also coincide.

For the matching of the distributions to be complete, the function $\mathcal{E}_b(t)$ of the boundary-layer distribution (25) should match on the MPEP the prefactor of the eikonal-approximation distribution $z^{-1/2}$ (23). Remarkably, they indeed have the same form, as functions of time, near $q_b(t)$. Therefore the parameters $\mathcal{Z}_1$ and $\mathcal{Z}_2$ allow one to determine $\mathcal{E}$ and s_m'', and vice versa, $\mathcal{E}$ and s_m'' give $\mathcal{Z}_1$ and $\mathcal{Z}_2$. With the appropriately defined parameters, not only the exponents but

also the prefactors of the boundary-layer and eikonal distributions fully match each other.

The function $p_{\rm opt}(t)$ exponentially decays with time, and therefore the term proportional to $p_{\rm opt}^{-2}(t)$ in $\mathcal{E}_b$ and $z^{-1/2}$ exponentially increases as $t\to\infty$. This leads to qualitatively different forms of the prefactor for different frequencies and strengths of the modulation. For $\Omega_F^2 s_m'' \ll l_D^2/\sigma_b^2(t)$, which corresponds to slow and not too strong modulation (see below), the term proportional to $p_{\rm opt}^{-2}$ in $\mathcal{E}_b$ is small in the whole harmonic region. Then the constant $\mathcal{Z}_2$ in $z(t)$ should be small as well. In this case the prefactor is determined by the constant $\mathcal{Z}_1$. This gives

$$\tilde{\mathcal{E}} = \mathcal{Z}_1^{-1/2}. \tag{27}$$

In the opposite case of very strong and/or higher-frequency modulation, where $\Omega_F^2 s_m'' \sim \Delta q^2/\sigma_b^2(t)$, the term proportional to $p_{\rm opt}^{-2}$ is much larger than $\sigma_b^2(t)$ in the whole harmonic region, and the constant $\mathcal{Z}_1$ in $z(t)$ can be disregarded. In this case

$$\tilde{\mathcal{E}}/\Omega_F\sqrt{s_m''} = \mathcal{Z}_2^{-1/2}. \tag{28}$$

Equation (25) describes also the intermediate case where the term proportional to $p_{\rm opt}^{-2}$ in $\mathcal{E}_b(t)$ and $z(t)$ is small in a part of the harmonic region sufficiently far from $q_b(t)$, but becomes large closer to q_b while still outside the layer $\sim l_D$. This regime corresponds to strong synchronization for comparatively weak driving. Here, both parameters $\mathcal{Z}_1$ and $\mathcal{Z}_2$ are important and can be used for matching, giving the same result. The corresponding analysis is provided in Appendix A.

As we will show, to calculate the escape rate in the regime of strong synchronization there is no need in finding the whole function $s(\phi)$ in the boundary-layer distribution, it is sufficient to know only s_m''. Equations (18) and (25) then provide the complete solution of the problem of escape.

V. TIME DEPENDENCE OF THE ESCAPE RATE

A. Adiabatic limit

Explicit expressions for the escape rate in the regime of strong synchronization can be obtained for comparatively weak or comparatively slow (adiabatic) modulation, where $s_m'' \sim |s_m| \gg D$ but

$$\Omega_F^2 s_m'' \ll R. \tag{29}$$

The results for comparatively weak modulation, $|s_m| \ll R$, should go over into the results [17], which were limited to this range, but included the strong-synchronization region $|s_m| \gg D$. This is demonstrated in Appendix A. We show that s_m'' found from Eqs. (21) and (25) by perturbation theory in the modulation amplitude A coincides with the result of Ref. [17].

Condition (29) can be met for large A, where $s_m'' \sim R$, provided the modulation frequency is small compared to the reciprocal relaxation time, $\omega_F t_r \sim \Omega_F \ll 1$. In this adiabatic regime the stable and unstable states $q_{a,b}^{\rm ad}(t)$ are the periodic solutions of the equation

$$K(q_{a,b}^{\rm ad}(t),t) = 0.$$

In the adiabatic approximation, escape happens very fast compared to the modulation period. This means that the escape trajectory can be calculated as if the force $K(q,t)$ did not depend on t explicitly. One can think then of a particle in the instantaneous potential well $U(q,t)$ [cf. Fig. 1(a)]. The intrawell distribution has the form

$$\rho(q,t) = [2\pi D\sigma_a^2(t)]^{-1/2} \exp\{-[U(q,t) - U(q_a^{\rm ad}(t),t)]/D\}, \tag{30}$$

where $\sigma_a^{-2}(t) = \partial_q^2 U(q,t)$, with the derivative evaluated for $q = q_a^{\rm ad}(t)$.

The adiabatic MPEP is given by the equation $\dot{q}_{\rm opt} = -K(q_{\rm opt}(t),t_m)$. The time t_m (i.e., the phase of the modulation $\phi_m = \omega_F t_m$) is found from the condition that the adiabatic barrier height of the potential $U(q,t)$,

$$\Delta U(t) = U(q_b^{\rm ad}(t),t) - U(q_a^{\rm ad}(t),t), \tag{31}$$

be minimal, $d\Delta U/dt = 0$ for $t = t_m$. The minimal barrier height gives the activation energy of escape,

$$R = \Delta U_m \equiv \Delta U(t_m).$$

The value of s_m'' can be obtained by matching the intrawell distribution (30) and the boundary-layer distribution (8). The matching is done most easily for sufficiently large $Q = q - q_b^{\rm ad}(t)$, so that $|Q| \gg l_D$ and $\mu_b(t_m)Q^2 \gg \Omega_F^2 s_m''$, and for $\delta t = t - t_m$ small compared to the modulation period τ_F but large compared to the typical relaxation time $\mu_b^{-1}(t_m)$. In this range, in Eq. (30)

$$U(q,t) - U(q_a^{\rm ad}(t),t) \approx \Delta U_m + \frac{1}{2}\Delta\ddot{U}_m\delta t^2 + \frac{1}{2}\mu_b Q^2,$$

where $\Delta\ddot{U}_m = d^2\Delta U/dt^2$, with the derivative calculated for $t = t_m$; here and below in this subsection for brevity we use μ_b for $\mu_b(t_m)$.

To find the boundary-layer distribution we note that, for the corresponding $\delta t, Q$, the integral over p in Eq. (6) can still be evaluated by the steepest descent method. However, in contrast to the analysis of Sec. IV B, the phase ϕ that provides the extremum to the integral is not equal to the optimal phase ϕ_m, which corresponds to the adiabatic MPEP $q_{\rm opt}(t)$. Indeed, the MPEP goes through a given $q = Q + q_b^{\rm ad}(t_m)$ at the time $t_{\rm opt}(Q)$ that differs from t_m by the relaxation time $\sim\mu_b^{-1}$. We have chosen δt so that $|t_{\rm opt}(Q) - t_m| \ll |\delta t|$.

A straightforward but somewhat tedious analysis shows that the major term in the phase difference is $\phi - \phi_m \approx \Omega_F\mu_b\delta t$. Then Eq. (6) gives

$$\rho(q,t) \approx (2\pi\mu_b)^{1/2}\mathcal{E}\exp\left\{-\frac{1}{D}\left[s_m + \frac{1}{2}(\mu_b Q^2 + \Omega_F^2\mu_b^2 s_m''\delta t^2)\right]\right\}.$$

By comparing this expression with Eq. (30) near q_b, t_m we obtain

$$\mathcal{E} = [4\pi^2 D\mu_b/|\mu_a|]^{-1/2}\, e^{-(\Delta U_m - s_m)/D},$$

$$s_m'' = \Delta\ddot{U}_m/\Omega_F^2\mu_b^2 \tag{32}$$

[here $\mu_i \equiv \mu_i(t_m)$, for $i=a,b$].

We note that the modulation frequency ω_F drops out from the expression for s_m'', because $\Omega_F \propto \omega_F$ while $\Delta\ddot{U} \propto \omega_F^2$. In Appendix B we show that the same expressions for the distribution parameters can be obtained by solving Eq. (21) for the prefactor.

Escape current

The expressions for the coefficients (32) allow evaluating the escape current $j(q,t)$ [Eq. (11)] in an explicit form. For $s_m'' \gg D$ the current has sharp peaks as function of time, i.e., escape is strongly synchronized. The peak shape can be found by extending the analysis of Sec. III B used to demonstrate the very onset of synchronization.

For ϕ_d close to $\phi_m - 2\pi k$ with integer k, the expression (11) for ϕ_d can be written as

$$\phi_d \approx \phi_m + \Omega_F \ln(x/x_k),$$

$$x_k = x_0 \exp(2\pi k/\Omega_F), \quad x_0 = p_{\rm opt}(t)Q/D, \tag{33}$$

where we used Eq. (24) for $p_{\rm opt}(t)$ [$x_k \equiv x_k(Q,t)$]. Expanding in Eq. (11) $s(\phi_d)$ near the minimum and using Eq. (32) we obtain

$$j(q,t) = W_m \sum\nolimits_k J_k(Q,t), \quad W_m = \frac{|\mu_a\mu_b|^{1/2}}{2\pi} e^{-R/D},$$

$$J_k = \int_0^\infty dx\, e^{-x} \exp\{-(\theta/2)[\ln(x/x_k)]^2\}, \tag{34}$$

where

$$\theta = \Omega_F^2 s_m''/D \sim \Omega_F^2 |s_m|/D. \tag{35}$$

The factor W_m in Eq. (34) is the Kramers escape rate in the stationary potential $U(q,t_m)$. Because of the modulation, the escape current (34) is a periodic sequence of sharp peaks. To show this we note first that, for any given time, the functions $x_k(Q,t)$ with different k are exponentially different, because $\Omega_F \ll 1$. Therefore J_k are also exponentially different. Only one J_k becomes large within a given period $(t, t+\tau_F)$. This happens in a narrow time interval where the corresponding $x_k \sim 1$ (see below). The periodicity of the current is a consequence of the relation $x_k(Q,t+\tau_F) = x_{k+1}(Q,t)$, which follows from Eq. (18).

The shape of the current peaks is determined by the parameter θ. For $\theta \ll 1$, the typical x_k that contribute to J_k in Eq. (34) are given by the condition $\theta \ln^2 x_k \lesssim 1$. For t close to t_m one can show from Eq. (17) with $K = K(q,t_m)$ that $p_{\rm opt}(t) = C\exp[-(t-t_m)\mu_b]$, with $C \sim \mu_b[q_b(t_m) - q_a(t_m)]$. Then from Eq. (33)

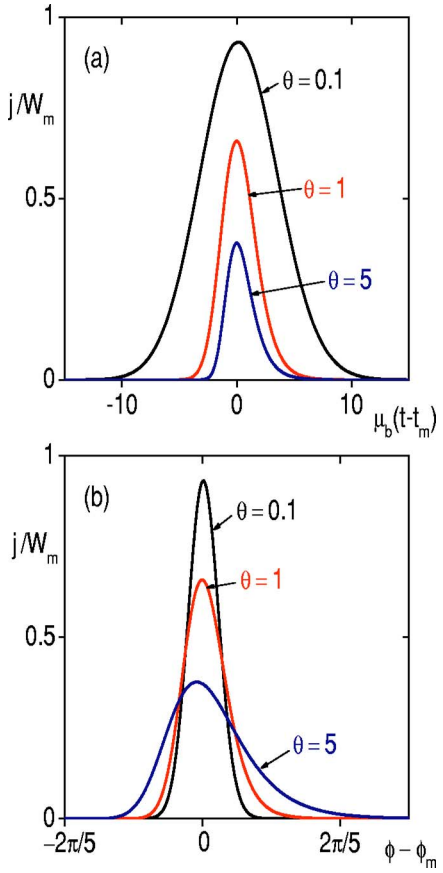

FIG. 2. (Color online) (a) Pulses of escape current in the adiabatic approximation as functions of time scaled by the relaxation time. With increasing parameter θ the pulses change from Gaussian to strongly asymmetric. (b) The same pulses as functions of time scaled by the modulation period $\phi = \omega_F t$.

$$x_k(t) \approx \exp[-(t-t_k)\mu_b], \quad t_k = t_m + k\tau_F, \tag{36}$$

with $k = 0, \pm 1, \ldots$ [we disregard the correction $\mu_b^{-1}\ln(QC/D)$ to t_k; it is of the order of the Suzuki time [26]]. Then the escape current near its maxima becomes

$$j(q,t) = W_m \sum\nolimits_k e^{-(t-t_k)^2 \Delta\ddot{U}_m/2D}, \quad \theta \ll 1. \tag{37}$$

The current pulses (37) have Gaussian form. They are centered at $t = t_k = t_m + k\tau_F$. The pulse width δt_w is determined by the noise intensity and the modulation frequency, $\delta t_w \sim (D/\Delta U_m)^{1/2}\tau_F$. We note that the condition $\theta \ll 1$ means that this width is much larger than the relaxation time of the system $\sim \mu_b^{-1}$ [cf. Fig. 2(a)]. Equation (37) corresponds to the fully adiabatic picture, where the escape rate is given by the instantaneous barrier height $\Delta U(t)$.

For larger θ, where $\theta \sim 1$, the pulse shape is no longer Gaussian. We emphasize that this happens where the modulation is still slow, $\Omega_F \ll 1$, and one would expect the adiabatic picture to fully apply.

The pulse shape can be found explicitly in the limit $\theta \gg 1$ but $\Omega_F \ll 1$. In this case J_k can be evaluated by the steepest descent method, giving

$$J_k(Q,t) \approx (2\pi/\theta)^{1/2} x_k \exp(-x_k). \tag{38}$$

As a function of time, J_k displays a peak where $x_k(t)=1$. The width of the peak $\delta t_w \sim \mu_b^{-1}$ is now independent of both the noise intensity and the modulation frequency. The peak is strongly asymmetric, because x_k depends on time exponentially [cf. Eq. (36)].

The evolution of the peak shape with varying parameter θ is demonstrated in Fig. 2. It is the same as for weak modulation [27], but the dependence of the parameters on the modulation amplitude is different, for strong modulation. Figure 2(b) shows that, with increasing modulation frequency, not only does the height of the peaks decrease, i.e., the modulation of the escape current becomes less pronounced, but also the width of the pulses with respect to the modulation period rapidly increases.

B. Nonadiabatic regime

The shape of the escape current peaks can be analyzed also for $\Omega_F \lesssim 1$, where the adiabatic approximation does not apply. Our analysis is based on Eqs. (11), (25), and (26). The function $p_{\rm opt}^{-2}(t) \propto \kappa_b^2(t,t')$ in Eq. (25) for $\mathcal{E}_b$ exponentially increases in time near q_b; therefore the term proportional to $p_{\rm opt}^{-2}$ in $\mathcal{E}_b$ and z becomes dominating before the MPEP reaches the diffusion region $|Q| \sim l_D$, and in Eqs. (11) and (25) $\mathcal{E}_b = \tilde{\mathcal{E}} D^{-1/2} [\Omega_F^2 s_m'' p_{\rm opt}^{-2}(t)]^{-1/2}$.

Integration over x in Eq. (11) can be done by the steepest descent method. Using Eq. (24) one can write in Eq. (11) $\phi_d - \phi_m = \Omega_F \ln[xD/Qp_{\rm opt}(t)]$. The major contribution to $j(q,t)$ near its maximum comes from the range $|\phi_d - \phi_m| \lesssim (D/\Omega_F^2 s_m'')^{1/2} \ll 1$. Expanding $s(\phi_d)$ to the second order in $\phi_d - \phi_m$ and performing integration over x we obtain from Eqs. (11) and (25)

$$j(q,t) = \frac{\mu_b(t)\tilde{\mathcal{E}} D^{1/2}}{\Omega_F \sqrt{s_m''}} e^{-R/D} \sum_{k=-\infty}^{\infty} x_k e^{-x_k},$$

$$x_k = x_0 \exp(2\pi k/\Omega_F), \quad x_0 = p_{\rm opt}(t) Q/D. \tag{39}$$

Note that here $p_{\rm opt}(t)$ can be smaller than $l_D/\sigma_b^2(t)$.

Equation (39) describes the escape rate in the whole region $\Omega_F^2 s_m'' \gg D$; it does not require the adiabatic approximation. The ratio $\tilde{\mathcal{E}}/\sqrt{s_m''}$ can be obtained from Eq. (28) by solving Eq. (21). In the adiabatic limit Eq. (39) gives the same result as Eq. (38). The current peaks (39) are strongly asymmetric. The current is maximal, for given Q, when $x_k=1$. The width of the current peaks is given by the reciprocal relaxation time $\sim \mu_b^{-1}$. The form of the current peaks is totally different from that of the diffusion current $-D\partial_Q \rho$ on the basin boundary $Q=0$. This current was studied in Refs. [18,19]. It can be easily obtained from Eqs. (6) and (25) with $Q=0$. The regime $\Omega_F^2 s_m''/D \ll 1$, where the current has the form (37), cannot be studied in the approximation [18] at all.

With increasing Ω_F the peaks of j (39) are smeared out and the escape synchronization is weakened. For $\Omega_F \gg 1$ the exponentially strong synchronization disappears. In addition to the fact that the width of the peaks $\bar{\mu}_b^{-1}$ becomes of the order of the interpeak distance τ_F for $\Omega_F \gtrsim 1$, s_m'' rapidly decreases with increasing ω_F for large Ω_F.

C. Nonlinear current propagation

In experiments the instantaneous escape rate can be measured as current $j(q,t)$ for a given q well behind the basin boundary $q_b(t)$, i.e., $q - q_b(t) \gg l_D$. When noise is weak, motion behind the basin boundary is practically noise-free ("deterministic"). Then the escape current is $j(q,t) = K(q,t)\rho(q,t)$. The function $\rho(q,t)$ can be related to the distribution $\rho(q_b(t)+Q,t)$ in the harmonic region where $Q \gg l_D$. The relation can be obtained from the Fokker-Planck equation with neglect of the diffusion term $\partial_t \rho + \partial_q [K(q,t)\rho] = 0$, and can be expressed in terms of the trajectories in the absence of noise $q_{\rm det}(t;t_0)$. A trajectory $q_{\rm det}$ is given by the equation

$$\partial_t q_{\rm det} = K(q_{\rm det}, t),$$

$$q_{\rm det}(t;t_0) = q, \quad q_{\rm det}(t_0;t_0) = q_b(t_0) + Q. \tag{40}$$

The boundary conditions in Eq. (40) follow from the fact that $q_{\rm det}(t;t_0)$ arrives at observation point q at time t and starts at point $q_b(t_0)+Q$ at time t_0. Equation (40) gives t_0 as a function of q,t. The distribution behind the boundary is

$$\rho(q,t) = \exp\left\{ -\int_{t_0}^{t} d\tau [\partial_q K(q,\tau)]_{\rm det} \right\} \rho_0(t_0), \tag{41}$$

where the derivative $\partial_q K$ is calculated along the trajectory $q_{\rm det}(t;t_0)$, and $\rho_0(t_0) = \rho(q_b(t_0)+Q, t_0)$.

The current $j(q,t)$ has a simple form for adiabatic modulation, $\Omega_F \ll 1$. In this case, as long as q is not too far from $q_b(t_m)$, one can calculate the trajectory $q_{\rm det}$ for the modulation phase that corresponds to $t=t_m$, where the current is close to maximum. This gives for $t_0 = t_0^{\rm ad}$ the expression

$$t_0^{\rm ad}(q,t) = t - \delta t_0^{\rm ad}(q), \quad \delta t_0^{\rm ad} = \int_{q_b(t_m)+Q}^{q} \frac{dq'}{K(q',t_m)}. \tag{42}$$

Equation (42) shows that there is a simple q-dependent shift between t and $t_0^{\rm ad}$, which is equal to the duration of deterministic motion from $q_b(t_m)+Q$ to the observation point q. We assume that this shift is small compared to the modulation period τ_F.

In the adiabatic approximation Eq. (41) is further simplified for t close to $t_m + k\tau_F$. In this case

$$\exp\left[-\int_{t_0}^{t} d\tau (\partial_q K)_{\rm det} \right] \approx \frac{K(q_b(t_m)+Q, t_m)}{K(q,t_m)} \approx \mu_b(t_m) Q/K(q,t_m),$$

where we have taken into account that $K(q_b(t_m),t_m) = \dot{q}_b(t_m) \propto \omega_F$ [in the case of additive modulation $K(q,t) = K_0(q) + F(t)$, we have $K(q_b,t_m)=0$]. Therefore, we obtain for the current in the adiabatic approximation

$$j^{\rm ad}(q,t) = j(Q, t_0^{\rm ad}). \tag{43}$$

Thus, in the adiabatic approximation the current near the peaks does not change shape but just shifts in phase, with the

phase shift described by Eq. (42). With increasing parameter θ [Eq. (35)] the current peaks change from Gaussian, for $\theta \ll 1$ [see Eq. (37)], to strongly asymmetric [see Eq. (38)]. The peaks are located at $t=t_k+\delta t_0^{\rm ad}$, with $t_k=t_m+k\tau_F$ [Eq. (36)]. We note that in Eq. (36) we disregarded a shift of t_k by the Suzuki time $\sim\mu_b^{-1}\ln(Q/l_D)$. This shift compensates the term in $\delta t^{\rm ad}$ [Eq. (42)] that logarithmically depends on Q, so that the overall position of the current peaks (37), (38), and (43) is independent of the matching point Q.

In the nonadiabatic case the difference $t-t_0$ depends not only on the observation point q, but also on time t. In addition, the factor that relates $\rho(q,t)$ and $\rho_0(t_0)$ in Eq. (41) becomes t dependent. Therefore, the overall shape of the current changes. However, the escape current has sharp peaks only where their width is small compared to the interpeak distance. From this point of view, the case of slow modulation is most interesting for studying the shape of escape current and synchronization of escape as a whole.

VI. PERIOD-AVERAGE ESCAPE RATE

In the range $s_m'' \sim |s_m| \gg D$, the period-average escape rate (12) is

$$\bar{W} = \nu \exp(-R/D), \quad \nu = \bar{\mu}_b \tilde{\mathcal{E}} D^{1/2}/2\pi\sqrt{s_m''}. \tag{44}$$

The prefactor ν can be expressed in terms of $\mathcal{Z}_2$ using Eq. (28), formally giving the result [18] even where the theory [18] does not apply.

The asymptotic technique developed in this paper allows obtaining the prefactor ν in several limiting cases. For comparatively weak modulation $D \ll |s_m| \ll R$, Eqs. (21) and (44), give the same result as in Ref. [17], with the scaling $\nu \propto (s_m'')^{-1/2} \propto A^{-1/2}$. Since the theory [17] covers the whole range $|s_m| \ll R$, a transition from the Kramers limit of no modulation to the case of arbitrarily strong modulation is now fully described.

In the whole range where the adiabatic approximation applies, $\Omega_F \ll 1$, from Eqs. (26) and (32) we obtain

$$\nu = (2\pi)^{-3/2} |\mu_a \mu_b|^{1/2} D^{1/2} \omega_F (\Delta \ddot{U}_m)^{-1/2} \tag{45}$$

where $\mu_{a,b}$ are calculated for $t=t_m$. Interestingly, ν [Eq. (45)] is independent of the modulation frequency.

VII. SCALING NEAR THE BIFURCATION POINT

Close to the bifurcational value of the modulation amplitude $A=A_c$ where the metastable and unstable states $q_{a,b}(t)$ merge, the escape rate displays system-independent features. As shown earlier [28], the activation energy R of the system scales as $R \propto \eta^{\xi}$, where $\eta \propto (A_c - A)$ is the reduced distance to the bifurcation point along the amplitude axis [see Eq. (48) below]. Three scaling regimes have been identified for R. With increasing modulation frequency ω_F or decreasing η, the critical exponent ξ changes from $\xi=3/2$ for stationary systems (adiabatic scaling) to $\xi=2$ (locally nonadiabatic scaling) and then back to $\xi=3/2$ (high-frequency scaling). Below we discuss scaling of the prefactor ν in these regimes.

A. Adiabatic scaling

We start the analysis with the limiting case of slow modulation $\omega_F t_r \ll 1$. In this case the adiabatic stable and unstable states $q_{a,b}^{\rm ad}(t)$ are given by the equation $K(q_{a,b}^{\rm ad}(t),t)=0$. The adiabatic critical amplitude $A_c^{\rm ad}$ is determined by the condition that the states $q_{a,b}^{\rm ad}(t)$ touch each other. This happens once per period, and we set $t=k\tau_F$ $(k=0,\pm1,\ldots)$ at this time. We also set $q_{a,b}^{\rm ad}(k\tau_F)=0$ for $A=A_c^{\rm ad}$. Expanding the Langevin equation of motion around this point, we obtain

$$\dot{q} = \alpha q^2 + \beta \delta A^{\rm ad} - \alpha\gamma^2(\omega_F t)^2 + f(t), \tag{46}$$

where $\alpha=(1/2)\partial_q^2 K$, $\beta=\partial_A K$, $\gamma^2=-(2\alpha\omega_F^2)^{-1}\partial_t^2 K$. Here all derivatives are evaluated at $q=t=0$, $A=A_c^{\rm ad}$; γ is independent of ω_F; it is assumed, without loss of generality, that $\alpha>0$; $\delta A^{\rm ad}=A-A_c^{\rm ad}$. The force $f(t)$ is a zero-mean white Gaussian noise, $\langle f(t)f(t')\rangle = 2D\delta(t-t')$.

The adiabatic approximation applies provided not only $t_r^{\rm ad}\omega_F \ll 1$, but also $\partial_t t_r^{\rm ad} \ll 1$, where $t_r^{\rm ad}(t)=(1/2)[(\alpha\gamma\omega_F t)^2 - \alpha\beta\delta A^{\rm ad}]^{-1/2}$ is the adiabatic relaxation time. The relaxation time strongly depends on t and diverges for $A \to A_c^{\rm ad}$ and $t \to 0$. The inequality $\partial_t t_r^{\rm ad} \ll 1$ is therefore the most restrictive condition on adiabaticity; it requires that $t_r^{\rm ad} \ll t_l$, where $t_l = (\alpha\gamma\omega_F)^{-1/2}$ is a new dynamical time scale [28]. The condition $t_r^{\rm ad} \ll t_l$ is equivalent to $\omega_F \ll |\beta\delta A^{\rm ad}|/\gamma$.

The problem of escape is simplified in the adiabatic regime [11,14,28–31]. For a periodically modulated system, from Eq. (46) we obtain $|\mu_a| = \mu_b = 2|\alpha\beta\delta A^{\rm ad}|^{1/2}$, $\Delta\ddot{U}_m = 4\omega_F^2\gamma^2|\alpha\beta\delta A^{\rm ad}|^{1/2}$. Then, from Eq. (45), the prefactor scales as $\nu \propto |\delta A^{\rm ad}|^{1/4}$. We note that in the adiabatic approximation ν decreases as A approaches the bifurcational value and, because escape is strongly synchronized, $\nu \propto D^{1/2}$.

B. Locally nonadiabatic scaling

The critical slowing down of the system motion makes the adiabatic approximation inapplicable in the region $|\delta A^{\rm ad}|/A_c^{\rm ad} \lesssim \Omega_F$, where the condition $t_r^{\rm ad} \ll t_l$ is violated. In this range we rewrite Eq. (46) in the form [28]

$$\dot{Q} = Q^2 - \tau^2 + 1 - \eta + \tilde{f}(\tau), \tag{47}$$

where $Q=\alpha t_l q$, $\tau = t/t_l$, $\dot{Q}=dQ/d\tau$, $\tilde{f}(\tau)=(\gamma\omega_F)^{-1}f(t_l\tau)$. The control parameter

$$\eta = \beta(\gamma\omega_F)^{-1}(A_c - A), \quad A_c \approx A^{\rm ad} + \gamma\omega_F/\beta, \tag{48}$$

is the distance to the true bifurcation point A_c, which is shifted from $A_c^{\rm ad}$ because of the slowing down of the system and the delayed response associated with it. For small driving frequencies $\omega_F t_r \ll 1$, where the local expansion (46) applies, the shift in the bifurcational amplitude is linear in frequency, as seen from Eq. (48).

For $\eta \ll 1$ the activation energy scales [28] as $R \propto \eta^2$. In this region the most probable escape path $Q_{\rm opt}(\tau), P_{\rm opt}(\tau)$ corresponding to Eq. (47) is given by

$$Q_{\rm opt}(\tau) = \tau - \eta\int_0^{\tau} d\tau_1 [1 - \sqrt{2}e^{-\tau_1^2}] e^{\tau^2-\tau_1^2},$$

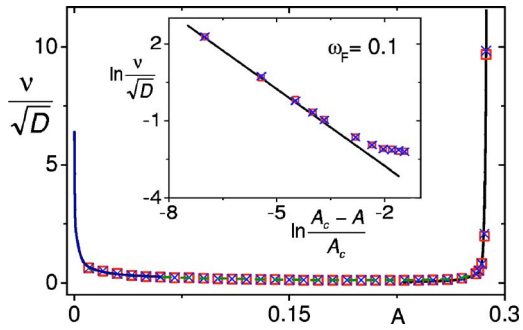

FIG. 3. (Color online) The prefactor ν in the average escape rate $\bar{W}$ [Eq. (44)]. The results refer to the model (52) with $\omega_F=0.1$ and describe escape in the regime of strong synchronization, where $\nu \propto D^{1/2}$. The solid line for small A shows the scaling $\nu \propto A^{-1/2}$ [17]. The solid lines for small $\delta A=A-A_c$ in the main figure and in the inset show the scaling (51). The dashed line shows the result of the numerical solution of Eq. (21). The squares and crosses show the results of Monte Carlo simulations for $R/D=5$ and 6, respectively.

$$P_{\rm opt}(\tau) = \eta e^{-\tau^2}/\sqrt{2}. \tag{49}$$

Using these expressions in Eq. (21), we obtain

$$z(\tau) = 4\pi\tilde{D}\int_{-\infty}^{\tau} d\tau_1 \exp(2\tau^2 - 2\tau_1^2). \tag{50}$$

Here $\tilde{D}=\alpha^{1/2}(\gamma\omega_F)^{-3/2}D$ is the intensity of the random scaled force $\tilde{f}(\tau)$. This gives

$$\nu = \nu_0 D^{1/2}|\delta A|^{-1}\omega_F^{5/4}, \quad \delta A = A - A_c, \tag{51}$$

where

$$\nu_0 = (32\pi^7)^{-1/4}|\alpha\gamma|^{1/4}\beta^{-1} = (64\pi^7\omega_F)^{-1/4}|\partial_t^2 K \partial_q^2 K|^{1/8}/|\partial_A K|.$$

From Eq. (51), the prefactor $\nu \propto |\delta A|^{-1}$ sharply increases as the modulation amplitude approaches A_c. This is qualitatively different from the decrease of ν in the adiabatic approximation. The result agrees with the numerical solution of Eqs. (21) and (44) for a model system shown in Fig. 3. The calculations in a broad range of A are also confirmed by Monte Carlo simulations, as discussed below.

C. High-frequency scaling

For high frequencies $\Omega_F \gg 1$, escape is not synchronized by the modulation. The prefactor in the escape rate is $\nu = |\bar{\mu}_a\bar{\mu}_b|^{1/2}/2\pi$, it is independent of the noise intensity D. Near the bifurcation point it scales as in stationary systems [11,29], where $\nu \propto |\delta A|^{1/2}$ and $R \propto |\delta A|^{3/2}$. We note that modulation is necessarily fast very close to the bifurcation point, because $|\bar{\mu}_{a,b}| \to 0$ for $A \to A_c$. Therefore the prefactor always goes to zero for $A \to A_c$. However, for small ω_F the corresponding region of δA is exponentially narrow [28]. The increase of ν with decreasing A_c-A in the locally nonadiabatic region does not contradict this picture because in this region $\nu \propto D^{1/2}$, whereas for effectively high-frequency modulation ν is independent of D.

VIII. RESULTS FOR A MODEL SYSTEM

To illustrate the findings, we consider a simple model system, a Brownian particle in a cubic potential subject to sinusoidal modulation. The Langevin equation is of the form

$$\dot{q} = K(q,t) + f(t), \quad K = q^2 - 1/4 + A\cos(\omega_F t), \tag{52}$$

with $f(t)$ being white Gaussian noise of intensity D.

A. The adiabatic regime

The adiabatic stable and unstable states of the system (52) in the absence of noise are $q_{a,b}^{\rm ad}(t) = \mp[1/4 - A\cos(\omega_F t)]^{1/2}$, and the adiabatic critical amplitude is $A_c^{\rm ad}=1/4$. The adiabatic barrier height is $\Delta U(t)=(4/3)[1/4-A\cos(\omega_F t)]^{3/2}$. Its minimum $\Delta U_m=(4/3)(1/4-A)^{3/2}$ is reached for $t_m=k\tau_F$, with $k=0,\pm 1,\ldots$.

The reduced curvature $\Omega_F^2 s_m''$ of the function $s(\phi)$ in the boundary-layer distribution at $\phi_m=\omega_F t_m$ is given by Eq. (32),

$$\Omega_F^2 s_m'' = (1/2)A\omega_F^2(1/4 - A)^{-1/2}. \tag{53}$$

Therefore the condition of strong but slow modulation $\Omega_F^2 s_m'' \ll D$, which must hold for the pulses of the escape current to be of Gaussian shape, takes the form

$$\omega_F^2 \ll D(1/4 - A)^{1/2}/A.$$

It becomes more and more restrictive for the modulation frequency as the modulation amplitude A approaches the adiabatic bifurcational value 1/4.

The prefactor ν of the period-average escape rate in the adiabatic limit for sufficiently strong modulation is given by Eq. (45). For our model it has a simple explicit form

$$\nu = (2\pi^{3/2})^{-1}D^{1/2}(1/4 - A)^{1/4}A^{-1/2}. \tag{54}$$

As expected, $\nu \propto A^{-1/2}$ for small amplitude, whereas close to the adiabatic bifurcation point $\nu \propto (A_c^{\rm ad} - A)^{1/4}$.

B. Locally nonadiabatic regime near the bifurcation point

As explained in Sec. VII, sufficiently close to the bifurcation point the adiabatic approximation breaks down. As a result, the bifurcation point A_c shifts away from $A_c^{\rm ad}$ (to higher amplitude, in our case). Close to A_c the pulses of escape current become strongly asymmetric, even though the modulation frequency is small. The scaling of the prefactor in the period-average escape rate also changes dramatically, from decreasing (as in the adiabatic approximation) to increasing for $A \to A_c$. From Eqs. (51) and (52)

$$\nu = (64\sqrt{2}\pi^7)^{-1/4}D^{1/2}|\delta A|^{-1}\omega_F^{5/4}. \tag{55}$$

The results on the prefactor for the discussed model system in the range $\omega_F t_r^{(0)} \ll 1$ are shown in Fig. 3 [$t_r^{(0)}$ is the relaxation time in the absence of modulation; for the model (52) $t_r^{(0)}=1$]. They refer to the modulation frequency $\omega_F=0.1$. The dependence of $\nu/\sqrt{D}$ on the modulation amplitude A is shown in the main part of the figure. The solid line for small A represents Eq. (54). The solid line close to the bifurcational amplitude $A_c \simeq 0.29$ is given by Eq. (55). The

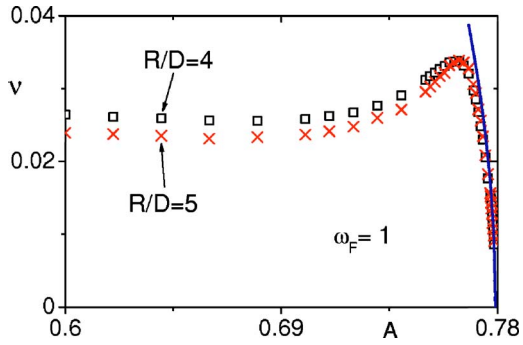

FIG. 4. (Color online) The prefactor ν in the average escape rate $\bar{W}$ (44) close to the bifurcation point $A=A_c$. The results refer to the model (52) with $\omega_F=1$. The squares and crosses show the results of Monte Carlo simulations for $R/D=4$ and 5, respectively. The solid line shows the asymptotics $\nu=|\bar{\mu}_a\bar{\mu}_b|^{1/2}/2\pi\propto(A_c-A)^{1/2}$.

dashed line for intermediate values of A is given by Eq. (44) with $\tilde{\mathcal{E}}/\sqrt{s_m''}$ [Eq. (28)] evaluated by numerically integrating Eq. (21). It is wel described by Eq. (54) for $A<0.2$. The analytical results agree with the results of simulations represented by squares and crosses. The inset shows in more detail the locally nonadiabatic scaling $\nu\propto|\delta A|^{-1}$ in the region near A_c.

The simulations have been done using the standard second-order integration scheme [32] for stochastic differential equations. The period-average escape rate was found as a reciprocal of the average dwell time of particles leaving the attraction basin. For each set of parameter values we accumulated $\sim 10^5$ escape events. The prefactor of the escape rate ν was evaluated as $\nu=\bar{W}\exp(R/D)$. The values of activation energy R were obtained independently by solving the appropriate instantonic problem. We checked previously [28] that these values agree extremely well with Monte Carlo simulations. For each value of A the noise intensity D was adjusted so as to keep R/D fixed at $R/D=5$ (squares) and 6 (crosses).

The results on the prefactor for higher modulation frequency are shown in Fig. 4. They were obtained in the same way as for lower frequency. It is seen from Fig. 4 that for the used model, already for $\omega_F t_r^{(0)}=1$ the amplitude dependence of the prefactor differs very significantly from the result of the adiabatic approximation. In particular, the prefactor displays the scaling behavior $\nu\propto(A_c-A)^{1/2}$ near the bifurcation point. It is independent of the noise intensity and is well described by the expression $\nu=|\bar{\mu}_a\bar{\mu}_b|^{1/2}/2\pi$.

IX. CONCLUSIONS

The results of this paper and the previous work allow us to draw a general scheme of the dependence of the rate of activated escape on the modulation parameters. This scheme is sketched in Fig. 5.

The weak-driving region corresponds to the case where the modulation-induced change of the activation energy of escape is small compared to the noise intensity D. In this region the major effect of modulation is weak "heating" of the system, which is quadratic in the modulation amplitude

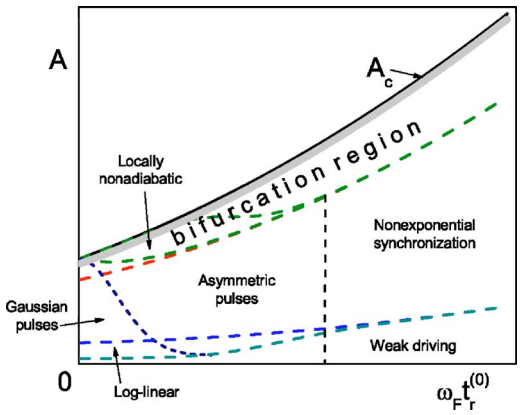

FIG. 5. (Color online) Different regions of escape behavior in modulated overdamped systems depending on the modulation frequency ω_F and amplitude A; $t_r^{(0)}$ is the relaxation time in the absence of modulation. The smeared boundaries between the regions are shown by dashed lines. The bold solid line indicates the bifurcational amplitude where the metastable state disappears. The shaded region below it indicates the range where the activation energy of escape $R\lesssim D$. The transition between the regions of exponentially strong and nonexponential synchronization occurs for $\omega_F t_r^{(0)}\sim 1$.

(for underdamped systems, the effective temperature depends on energy [10,33]). Escape is not synchronized by the modulation. The width of this region along the amplitude axis is proportional to D for low frequencies and becomes proportional to $\omega_F D^{1/2}$ for large $\Omega_F\sim\omega_F t_r$.

Synchronization emerges once the magnitude of the oscillations of the "instantaneous" activation energy $|s_m|$ becomes much larger than D. There is a broad region of modulation amplitudes where $|s_m|\propto A$ and the logarithm of the period-average escape rate $\bar{W}$ is linear in A, too [17]. This log-linear region in Fig. 5 is bounded on the large-A side by the condition $A/A_c\ll 1$, where A_c is the bifurcational value of A. Strong synchronization occurs for small frequencies $\Omega_F\ll 1$. Here, the escape current has peaks with width much smaller than the modulation period. The prefactor ν in the period-average escape rate scales as $(D/A)^{1/2}$.

Synchronization persists for higher modulation amplitudes. The shape of the peaks of escape current is Gaussian for $\Omega_F^2 s_m''\ll D$, and their width is $\sim(D/s_m'')^{1/2}\tau_F$. For higher frequencies, the peaks become strongly asymmetric and non-Gaussian, with width $\sim t_r$. In the log-linear region the boundary between the two types of peaks is $\omega_F\propto A^{-1/2}$.

For high modulation frequencies, $|s_m|$ becomes small and exponentially strong synchronization of escape disappears. The escape current is still modulated in time, of course, but generally it does not have a shape of sharp narrow peaks even for small noise intensity.

Of special interest is the bifurcation region, because there the dynamics and fluctuations display system-independent features. The region is determined by the condition $|A_c-A|\ll A_c$, as shown in Fig. 5. In this region, in the adiabatic approximation the boundary of the range where escape current peaks are Gaussian has the form $\omega_F\propto|A_c-A|^{1/4}$.

Close to A_c, where $(A_c-A)/A_c\Omega_F\sim 1$, the adiabaticity is broken. This condition and the condition $\Omega_F\ll 1$ determine

the boundary of the locally nonadiabatic region. Inside this region the escape current has the form of asymmetric narrow peaks. Special scaling is displayed for $(A_c-A)/A_c\Omega_F \ll 1$. Here, the activation energy of escape scales with the distance to the bifurcation amplitude A_c as $(A_c-A)^2$, whereas the prefactor in the period-average escape rate is proportional to $(A_c-A)^{-1}$. Because of the slowing down near the bifurcation point, the locally nonadiabatic behavior and synchronization of escape disappear for small A_c-A, which determines the high-A region boundary. This boundary is very close to A_c for small Ω_F, but for higher Ω_F the region of locally nonadiabatic behavior shrinks and ultimately disappears. Outside this region on the high-ω_F side, for A close to A_c the prefactor ν scales as $\nu \propto (A_c-A)^{1/2}$.

In conclusion, we have obtained a general solution of the problem of noise-induced escape in periodically modulated overdamped systems. For small ω_F the pulses of escape current are exponentially sharp and change with increasing ω_F from Gaussian to strongly asymmetric. For large ω_F exponential current modulation disappears. The prefactor ν in the period-average escape rate is a strongly nonmonotonic function of the modulation amplitude A for low frequencies. It first drops with increasing A to $\nu \propto (D/A)^{1/2}$ [17], then varies with A smoothly [18,19], and then sharply increases, $\nu \propto D^{1/2}/(A_c-A)$ near the bifurcation amplitude A_c. We found three scaling regimes near A_c, where $\nu \propto (A_c-A)^{\zeta}$ with $\zeta = 1/4,\ -1$, or $1/2$. The widths of the corresponding scaling ranges strongly depend on the modulation frequency.

ACKNOWLEDGMENTS

We are grateful to V. N. Smelyanskiy for the discussion. This research was supported in part by the NSF Grant No. DMR-0305746.

APPENDIX A: DISTRIBUTION MATCHING FOR DYNAMICALLY WEAK MODULATION

In this appendix we study, using our general approach, the case of moderately weak modulation and compare the results to the previous work [17]. Following Ref. [17] we assume that the force $K(q,t)=-U_{0q}+F(t)$, where $U_0(q)$ is the metastable potential in the absence of modulation (in this appendix we use the notation $f_q \equiv \partial_q f$). The force $F(t+\tau_F)=F(t)$ is dynamically weak. This means that it weakly disturbs the motion in the absence of fluctuations. Yet it may strongly change the escape rate, because there it is compared with the small noise intensity.

The distribution ρ inside the attraction basin can be found by calculating the action $S(q,t)$ in Eq. (14) to the first order in F. From Eqs. (15) and (16) S can be written in a standard way as an integral of the Lagrangian L,

$$S(q,t) = \int_{-\infty}^{t} d\tau\, L(q,\dot{q};\tau), \quad L = \frac{1}{4}[\dot{q} - K(q,t)]^2. \quad \text{(A1)}$$

The linear in F correction to S can be obtained by integrating the term proportional to F along the optimal escape path $q_0(t)$ in the absence of driving, $\dot{q}_0=p_0=U_{0q}(q_0)$. This gives

$$S(q,t) = U_0(q) - U_0(q_{a0}) + s(q,t),$$

$$s(q,t) = -\int_{-\infty}^{t} d\tau\, \dot{q}_0(\tau)F(\tau), \quad \text{(A2)}$$

where the optimal path is chosen so that $q_0(t)=q$, and q_{a0} is the stable state $q_a(t)$ in the limit $F=0$, with $U_{0q}(q_{a0})=0$; similarly, we use below q_{b0} as the basin boundary for $F=0$, with $U_{0q}(q_{b0})=0$. The quantity $\chi(t)=-\dot{q}_0(t)$ determines the field-induced change of the logarithm of the escape rate, and therefore was called logarithmic susceptibility.

Equation (A2) allows one to match the intrawell distribution $\rho(q,t)=|\mu_{a0}/2\pi D|^{1/2}\exp[-S(q,t)/D]$ to the boundary-layer distribution (6)–(8) for

$$-Q = q_{b0} - q \gg |s(q,t)/\mu_{b0}|^{1/2}, l_D \quad \text{(A3)}$$

[here $\mu_{i0} \equiv -U_{0qq}(q_{i0})$ with $i=a,b$]. In the range (A3) the integral over p [Eq. (6)] can be evaluated by the steepest descent, giving $\rho(q,t) \approx \mathcal{E}(2\pi\mu_{b0})^{1/2}\exp[-s(\phi)/D]$, with $\phi = (\omega_F/\mu_{b0})\ln(-Q/l_D)+\omega_F(t-t')$. The exponent of this boundary-layer distribution coincides with $-s(q,t)/D$ in the range (A3) if we set [17]

$$s(\phi) = \sum_n \tilde{\chi}(n\omega_F)F_n e^{in\phi},$$

$$\tilde{\chi}(\omega) = -\int_{-\infty}^{+\infty} dt\, \dot{q}_0(t)e^{i\omega t}. \quad \text{(A4)}$$

Here F_n are Fourier components of $F(t)$. Matching the prefactors in the intrawell and boundary-layer distributions gives

$$\mathcal{E} = \frac{1}{2\pi}|\mu_{a0}\mu_{b0}|^{1/2}\exp[-\Delta U_0/D]. \quad \text{(A5)}$$

We emphasize that the matching has been done not only far from the diffusion region, but also in the range (A3), that is, much further away from the boundary than diffusion length l_D, in the regime of strong synchronization $|s_m| \gg D$.

We will show now that the alternative approach of Sec. IV gives the same result in the case of strong synchronization $|s_m| \gg D$. To do this we have to solve the equation for the prefactor (21) to the first order in F, which in turn requires finding the first-order corrections to the optimal path q_1, p_1. Linearizing the first of Eqs. (17), one obtains

$$\dot{q}_1 = K_{0q}q_1 + F(t) + 2p_1. \quad \text{(A6)}$$

Here $K_{0q}(q) \equiv -U_{0qq}(q)$, and the derivative is evaluated for the zeroth-order optimal path, $q=q_0(t)$. The correction to the momentum, $p_1 \equiv \partial S/\partial q - p_0$, from Eq. (A2) is

$$p_1 = -K_{0q}q_1 - F(t) + \frac{1}{\dot{q}_0(t)}\int_{-\infty}^{t} d\tau\, \dot{q}_0(\tau)\dot{F}(\tau). \quad \text{(A7)}$$

To obtain Eq. (A7), we used the fact that $q_0(t)=q$, and therefore $\partial q_0(\tau)/\partial q = \dot{q}_0(\tau)/\dot{q}_0(t)$. We also took into account that $p_1(t) \to 0$ for $t \to -\infty$.

In the absence of driving the prefactor is constant, and the function $z(t)$ from Eq. (21) is determined by the initial con-

dition (22), $z=z_0=2\pi D/|\mu_{a0}|$. Let $z=z_0+z_1$, where z_1 is a correction proportional to F. The linearized Eq. (21) is

$$\ddot{z}_1 - 2K_{0q}\dot{z}_1 = 2z_0K_{0qq}(\dot{q}_1 - p_1). \tag{A8}$$

From Eqs. (A6)–(A8),

$$\dot{z}_1 = \frac{2z_0}{\dot{q}_0^2(t)}\int_{-\infty}^{t} d\tau\, \dot{q}_0(\tau)\dot{F}(\tau)[K_{0q}(q_0(t)) - K_{0q}(q_0(\tau))]. \tag{A9}$$

To find the parameters s_m'' and $\mathcal{E}$ of the boundary-layer distribution (25) and (26) we need to find z_1 close to q_{b0}, i.e., for $t\to\infty$. It follows from the results of Sec. III that, for strong modulation, in this range

$$\dot{z} \approx 2\mu_{b0}D\mathcal{Z}_2\dot{q}_0^{-2}(t), \tag{A10}$$

where we used that $p_0=\dot{q}_0$, $\dot{p}_0=-\mu_{b0}p_0$. Before we compare this expression with Eq. (A9) we note that the condition that s, as given by Eq. (A4), is minimal for $\phi=\phi_m$ corresponds to

$$\int_{-\infty}^{\infty} dt\, \dot{q}_0(t)\dot{F}(t) = 0.$$

This condition describes synchronization of the most probable escape path by the modulation. In the absence of modulation $q_0(t-t_c)$ is a MPEP for any t_c. Modulation lifts the time degeneracy; only one MPEP per period provides a minimum to s. As a consequence, the first integral in Eq. (A9) goes to zero for $t\to\infty$. Then from Eqs. (A9) and (A10) we obtain, taking into account that $\dot{q}_0=-K_0$,

$$\mathcal{Z}_2 = -\frac{2\pi}{|\mu_{a0}\mu_{b0}|}\int_{-\infty}^{\infty} dt\, \dot{q}_0(t)\ddot{F}(t). \tag{A11}$$

It follows from Eq. (A4) that $\mathcal{Z}_2=2\pi\omega_F^2 s_m''/|\mu_{a0}\mu_{b0}|$. Taking into account Eqs. (28) and (26), we obtain the same result for the prefactor in the boundary-layer distribution as Eq. (A5). We note that this result refers to the case of comparatively strong modulation $|s_m|\gg D$, and is obtained by matching the intrawell and boundary-layer distributions not in the region (A3) [17], but closer to the basin boundary, where $|s_m| \gg \mu_b Q^2$.

APPENDIX B: NONADIABATIC CORRECTIONS FOR SLOW MODULATION

In this appendix we show an alternative approach to the analysis of adiabatically slow modulation. By treating time variation of the modulation as a perturbation, we find the most probable escape path and also solve Eq. (21) for the auxiliary function z and obtain the constant $\mathcal{Z}_2$, [cf. Eq. (23)]. This provides an alternative way of finding the parameters of the boundary-layer distribution and also gives an insight into the actual dynamics of escape for slow modulation.

The small parameter of the slow-modulation theory is the reduced frequency $\omega_F t_r \ll 1$. The typical duration of escape is the relaxation time $\sim t_r$; it is much smaller than the modulation period $\tau_F=2\pi/\omega_F$. Escape is most likely to happen once per period, for the modulation phase $\phi_m=\omega_F t_m$ (which, as we show, corresponds to the minimal barrier height; t_r is the adiabatic relaxation time for $t=t_m$). For t close to t_m we can expand the force in the form

$$K(q,t) = K_0(q) + F_1(q,t) + F_2(q,t), \tag{B1}$$

where $K_0(q)\equiv K(q,t_m)$, $F_1(q,t)\equiv K_t(q,t_m)(t-t_m)$, $F_2(q,t) \equiv (1/2)K_{tt}(q,t_m)(t-t_m)^2$ (here and below $f_t\equiv\partial_t f$, $f_q\equiv\partial_q f$). Thus, K_0 represents a stationary force, and F_1 and F_2 are the time-dependent corrections of first and second order in $\omega_F t_r$.

To zeroth order in $\omega_F t_r$, the positions of the stable state q_a and basin boundary q_b of the system are the solutions q_{a0} and q_{b0} of the adiabatic equation $K_0(q)=0$ with $\mu_{a0}<0$ and $\mu_{b0}>0$, respectively, where $\mu_{i0}=K_{0q}(q_{i0})$ $(i=a,b)$. The parameters μ_{i0} characterize the relaxation rate of the system. We emphasize that, in contrast to Appendix A where K_0 referred to the system in the absence of modulation, here K_0 and the parameters $q_{a,b}, \mu_{a,b}$ are calculated for strong modulation but at a specific instant of time t_m.

Because of the time-dependent terms in K, the positions q_i $(i=a,b)$ acquire corrections $q_{i1,2}$ of the first and second order in $\omega_F t_r$, so that $q_i=q_{i0}+q_{i1}+q_{i2}$. They can be found from the equation $\dot{q}_i=K(q_i,t)$ and have the form

$$q_{i1} = -\left[\frac{F_{1t}}{\mu_{i0}^2} + \frac{F_1}{\mu_{i0}}\right]_{q_{i0}}, \quad i=a,b, \tag{B2}$$

and

$$q_{i2} = \left[-\frac{5}{2}\frac{K_{0qq}F_{1t}^2}{\mu_{i0}^5} + \frac{3F_{1t}F_{1qt}}{\mu_{i0}^4} - \frac{F_{2tt}}{\mu_{i0}^3} - \frac{2K_{0qq}F_{1t}F_1}{\mu_{i0}^4} + \frac{3F_{1qt}F_1}{\mu_{i0}^3} - \frac{F_{2t}}{\mu_{i0}^2} - \frac{1}{2}\frac{K_{0qq}F_1^2}{\mu_{i0}^3} + \frac{F_{1q}F_1}{\mu_{i0}^2} - \frac{F_2}{\mu_{i0}}\right]_{q_{i0}}, \quad i=a,b. \tag{B3}$$

We now consider corrections to the MPEP. For K given by Eq. (B1) it is natural to seek the solution of Eqs. (17) in the form $q=q_0+q_1+q_2$, $p=p_0+p_1+p_2$. To zeroth order in ω_F the MPEP is given by the equation

$$\dot{q}_0 = p_0 = -K_0(q_0).$$

The first-order corrections q_1, p_1 satisfy Eq. (A6) with $F=F_1$ and with the boundary conditions $q_1\to q_{a1}$ at $t\to-\infty$ and $q_1\to q_{b1}$ at $t\to\infty$. In the second order

$$\dot{q}_2 = K_{0q}q_2 + \frac{1}{2}K_{0qq}q_1^2 + F_{1q}q_1 + F_2 + 2p_2 \tag{B4}$$

with $q_2\to q_{a2}$ at $t\to-\infty$ and $q_2\to q_{b2}$ at $t\to\infty$. Here and below the functions K_0 and $F_{1,2}$ and their derivatives are calculated along the zeroth-order MPEP $q_0(t)$.

From the expression for the action (A1) with the force (B1) we obtain, similarly to Eq. (A7),

$$p_1 = -K_{0q}q_1 - F_1 + \frac{1}{\dot{q}_0(t)}\int_{-\infty}^{t} d\tau\, \dot{q}_0 F_{1\tau}.$$

Using this expression and Eq. (17), we further obtain

$$\dot{q}_1 - p_1 = \frac{1}{\dot{q}_0(t)} \int_{-\infty}^{t} d\tau\, \dot{q}_0 F_{1\tau}. \tag{B5}$$

The momentum $p_1 \to 0$ at $t \to \pm\infty$; therefore Eq. (B5) requires that

$$\frac{1}{\dot{q}_0(t)} \int_{-\infty}^{t} d\tau\, \dot{q}_0 F_{1\tau} \to \begin{cases} \dot{q}_{a1}, & t \to -\infty, \\ \dot{q}_{b1}, & t \to \infty, \end{cases} \tag{B6}$$

where $\dot{q}_{a1,b1}$ are given by Eq. (B2).

For $t \to -\infty$ the condition (B6) is met; hence the choice of the lower limit of integration. To consider the $t \to +\infty$ limit we write the left-hand side of Eq. (B6) as

$$\frac{1}{\dot{q}_0(t)} \int_{-\infty}^{\infty} d\tau\, \dot{q}_0 F_{1\tau} - \frac{1}{\dot{q}_0(t)} \int_{t}^{\infty} d\tau\, \dot{q}_0 F_{1\tau}.$$

For $t \to \infty$ the second term goes to $\dot{q}_{b1}$. Therefore to satisfy the condition (B6) we must have

$$\int_{-\infty}^{\infty} d\tau\, \dot{q}_0 F_{1\tau} = \int_{q_{a0}}^{q_{b0}} dq\, F_{1\tau}(q) = 0. \tag{B7}$$

In changing the integration variable we used that F_{1t} does not depend on t explicitly.

The condition (B7) is equivalent to the requirement that the adiabatic barrier height

$$\Delta U(t) = \int_{q_a(t)}^{q_b(t)} dq [K_0(q) + F_1(q,t) + F_2(q,t)] \tag{B8}$$

be minimal, $d\Delta U/dt = 0$, to the first order in ω_F.

We note that the condition (B7) is invariant with respect to time shift of the MPEP $q_0(t) \to q_0(t - t_c)$, with an arbitrary t_c. However, it does specify the modulation phase $\phi_m = \omega_F t_m$ when escape is most likely to occur.

The term in the action of second order in $\omega_F t_r$ has the form

$$S_2(q,t) = \frac{1}{4} \int_{-\infty}^{t} d\tau (\dot{q}_1 - K_{0q} q_1 - F_1)^2 + \int_{-\infty}^{t} d\tau\, \dot{q}_0 \left(\dot{q}_2 - K_{0q} q_2 - \frac{1}{2} K_{0qq} q_1^2 - F_{1q} q_1 - F_2 \right).$$

Using this equation to calculate $p_2 = \partial_q S_2$, we obtain from Eq. (B4)

$$\dot{q}_2 - p_2 = \frac{1}{\dot{q}_0(t)} \int_{-\infty}^{t} d\tau\, \dot{q}_0 u(\tau),$$

$$u(t) = F_{1qt} q_1 + F_{2t} + (\dot{q}_1 - p_1)(K_{0qq} q_1 + F_{1q}). \tag{B9}$$

Using Eq. (B3), one can check that (B9) satisfies the boundary condition $q_2 \to q_{a2}$, $p_2 \to 0$ for $t \to -\infty$. To satisfy the boundary condition at $t \to +\infty$ we must require that

$$\int_{-\infty}^{\infty} d\tau\, \dot{q}_0 u(\tau) = 0. \tag{B10}$$

The integral (B10) depends on the position t_c of the "center" of the MPEP $q_0(t - t_c)$ and thus specifies this position. Equations (B7) and (B10) fully determine both the phase of the modulation where escape is most likely to occur and the MPEP as a function of time.

We are now in a position to develop a perturbation theory for the function $z(t)$, which should be calculated along the MPEP from Eq. (21). The parameter of interest $\mathcal{Z}_2$ is determined by the asymptotic behavior of z for $t \to \infty$: this is the coefficient at the diverging term $D p_0^{-2}(t)$ in $z(t)$ [cf. Eq. (23)]. As we will see, $\mathcal{Z}_2 \propto \omega_F^2$, and therefore we need to find z to second order in $\omega_F t_r$. Respectively, we seek z in the form $z = z_0 + z_1 + z_2$, with $z_j \propto [\omega_F t_r]^j$ $(j = 0, 1, 2)$.

The initial conditions for z_j follow from Eq. (22). The function $\sigma_a^2(t)$ in Eq. (22) is a periodic solution of the equation $\dot{\sigma}_a^2 = 2\mu_a \sigma_a^2 + 2$, which can be easily solved by perturbation theory in $\omega_F t_r$. To zeroth order $(\sigma_a^2)_0 = 1/|\mu_{a0}|$ and $z_0 = 2\pi D/|\mu_{a0}|$.

From Eq. (21), the equation for z_1 has the form

$$\ddot{z}_1 - 2K_{0q}\dot{z}_1 = 2z_0[K_{0qq}(\dot{q}_1 - p_1) + F_{1qt}].$$

This equation differs from Eq. (A8) by the term F_{1qt}, which allows for q dependence of the perturbation force. The left-hand side can be written as $(1/\dot{q}_0^2) d(\dot{z}_1 \dot{q}_0^2)/dt$, which immediately gives

$$\dot{z}_1 \dot{q}_0^2 = 2z_0 \int_{-\infty}^{t} d\tau\, \dot{q}_0^2 [K_{0qq}(\dot{q}_1 - p_1) + F_{1q\tau}] = 2z_0 \dot{q}_0 [K_{0q}(\dot{q}_1 - p_1) + F_{1t}]. \tag{B11}$$

Here we have taken into account the initial condition for z_1 for $t \to -\infty$ and also used the relation

$$\frac{d}{dt}(\dot{q}_1 - p_1) = K_{0q}(\dot{q}_1 - p_1) + F_{1t}, \tag{B12}$$

which follows from Eq. (B5). Taking into account that $\dot{q}_1, p_1, F_{1t}$ do not diverge for $t \to \infty$, we see from Eq. (B11) that $\dot{z}_1(t)\dot{q}_0^2 \to 0$ as $t \to +\infty$. Therefore z_1 does not contain a term proportional to $\exp(2\mu_{b0} t) \propto p_0^{-2}(t)$ for $t \to \infty$, and as a consequence it does not contribute to $\mathcal{Z}_2$.

In the second order, from Eq. (21) we have

$$\ddot{z}_2 - 2K_{0q}\dot{z}_2 = v(t), \tag{B13}$$

where

$$v(t) = 2z_0[K_{0qq}(\dot{q}_2 - p_2) + (K_{0qqq} q_1 + F_{1qq})(\dot{q}_1 - p_1) + F_{1qqt} q_1 + F_{2qt}] + 2\dot{z}_1(K_{0qq} q_1 + F_{1q}) + 2z_1[K_{0qq}(\dot{q}_1 - p_1) + F_{1qt}]. \tag{B14}$$

The left-hand side of Eq. (B13) is $(1/\dot{q}_0^2) d(\dot{z}_2 \dot{q}_0^2)/dt$, and therefore

$$\dot{z}_2(t)\dot{q}_0^2(t) = \int_{-\infty}^{t} d\tau\, \dot{q}_0^2 v(\tau). \tag{B15}$$

A cumbersome calculation, which involves integration by parts using conditions (B7) and (B10) and Eqs. (B2), (B4), (B5), and (B9), shows that, as $t \to +\infty$, the integral in the right-hand side of Eq. (B15) tends to a constant

$$C = 2z_0\left[-\int_{-\infty}^{\infty} d\tau\, \dot{q}_0 F_{2tt} + \frac{[F_{1t}(q_{b0})]^2}{\mu_{b0}} - \frac{[F_{1t}(q_{a0})]^2}{\mu_{a0}} \right]. \tag{B16}$$

Equation (B16) is the central result of this appendix. It follows from this equation and the fact that the singular part of z behaves as $\exp(2\mu_{b0}t)$ for $t \to \infty$ that

$$\mathcal{Z}_2 = D^{-1} \lim_{t\to\infty} z(t) p_0^2(t) = \frac{C}{2\mu_{b0}D}.$$

On the other hand, from Eqs. (B8) and (B16) we obtain

$$\Delta\ddot{U}(t_m) = \frac{C}{2z_0} = \frac{C|\mu_{a0}|}{4\pi D}.$$

Therefore

$$\mathcal{Z}_2 = 2\pi\Delta\ddot{U}(t_m)/|\mu_{a0}\mu_{b0}|,$$

which coincides with the result of Eqs. (28) and (32).

[1] H. Kramers, Physica (Utrecht) **7**, 240 (1940).
[2] J. S. Aldridge and A. N. Cleland, Phys. Rev. Lett. **94**, 156403 (2005).
[3] C. Stambaugh and H. B. Chan, e-print cond-mat/0504791.
[4] Y. Yu and S. Han, Phys. Rev. Lett. **91**, 127003 (2003).
[5] A. Wallraff, A. Lukashenko, J. Lisenfeld, A. Kemp, M. V. Fistul, Y. Koval, and A. V. Ustinov, Nature (London) **425**, 155 (2003).
[6] I. Siddiqi, R. Vijay, F. Pierre, C. M. Wilson, M. Metcalfe, C. Rigetti, L. Frunzio, and M. H. Devoret, Phys. Rev. Lett. **93**, 207002 (2004).
[7] W. Wernsdorfer, E. B. Orozco, K. Hasselbach, A. Benoit, B. Barbara, N. Demoncy, A. Loiseau, H. Pascard, and D. Mailly, Phys. Rev. Lett. **78**, 1791 (1997); W. T. Coffey, D. S. F. Crothers, J. L. Dormann, Yu. P. Kalmykov, E. C. Kennedy, and W. Wernsdorfer, *ibid.* **80**, 5655 (1998).
[8] R. H. Koch, G. Grinstein, G. A. Keefe, Yu Lu, P. L. Trouilloud, W. J. Gallagher, and S. S. P. Parkin, Phys. Rev. Lett. **84**, 5419 (2000).
[9] E. B. Myers, F. J. Albert, J. C. Sankey, E. Bonet, R. A. Buhrman, and D. C. Ralph, Phys. Rev. Lett. **89**, 196801 (2002).
[10] M. H. Devoret, D. Esteve, J. M. Martinis, A. Cleland, and J. Clarke, Phys. Rev. B **36**, 58 (1987); E. Turlot, S. Linkwitz, D. Esteve, C. Urbina, M. H. Devoret, and H. Grabert, Chem. Phys. **235**, 47 (1998).
[11] J. Kurkijärvi, Phys. Rev. B **6**, 832 (1972).
[12] For a recent review, see S. M. Soskin, R. Mannella, and P. V. E. McClintock, Phys. Rep. **373**, 247 (2003).
[13] C. R. Doering and J. C. Gadoua, Phys. Rev. Lett. **69**, 2318 (1992).
[14] M. Bier, Phys. Rev. E **71**, 011108 (2005).
[15] M. I. Dykman and D. Ryvkine, Phys. Rev. Lett. **94**, 070602 (2005).
[16] M. I. Dykman, B. Golding, L. I. McCann, V. N. Smelyanskiy, D. G. Luchinsky, R. Mannella, and P. V. E. McClintock, Chaos **11**, 587 (2001), and references therein.
[17] V. N. Smelyanskiy, M. I. Dykman, and B. Golding, Phys. Rev. Lett. **82**, 3193 (1999).
[18] J. Lehmann, P. Reimann, and P. Hänggi, Phys. Rev. Lett. **84**, 1639 (2000); Phys. Rev. E **62**, 6282 (2000).
[19] R. S. Maier and D. L. Stein, Phys. Rev. Lett. **77**, 4860 (1997); **86**, 3942 (2001).
[20] R. Graham and T. Tél, Phys. Rev. Lett. **52**, 9 (1984); J. Stat. Phys. **35**, 729 (1984); Phys. Rev. A **31**, 1109 (1985).
[21] M. V. Berry, Adv. Phys. **35**, 1 (1976).
[22] D. Ludwig, SIAM Rev. **17**, 605 (1975).
[23] M. I. Freidlin and A. D. Wentzell, *Random Perturbations in Dynamical Systems*, 2nd ed. (Springer-Verlag, New York, 1998).
[24] D. Ryter and P. Jordan, Phys. Lett. **104A**, 193 (1984).
[25] In Ref. [15] we used the notation $z_{1,2}$ for these constants. In the present paper $z_{1,2}$ denote the first- and second-order corrections to z in the asymptotic regimes discussed in Appendices A and B.
[26] M. Suzuki, J. Stat. Phys. **16**, 11 (1977); **16**, 477 (1977).
[27] V. N. Smelyanskiy, M. I. Dykman, H. Rabitz, B. E. Vugmeister, S. L. Bernasek, and A. B. Bocarsly, J. Chem. Phys. **110**, 11488 (1999).
[28] M. I. Dykman, B. Golding, and D. Ryvkine, Phys. Rev. Lett. **92**, 080602 (2004); D. Ryvkine, M. I. Dykman, and B. Golding, Phys. Rev. E **69**, 061102 (2004).
[29] M. I. Dykman and M. A. Krivoglaz, Physica A **104**, 480 (1980).
[30] R. H. Victora, Phys. Rev. Lett. **63**, 457 (1989).
[31] O. A. Tretiakov, T. Gramespacher, and K. A. Matveev, Phys. Rev. B **67**, 073303 (2003); O. A. Tretiakov and K. A. Matveev, *ibid.* **71**, 165320 (2005).
[32] R. Mannella, Int. J. Mod. Phys. C **13**, 1177 (2002).
[33] A. I. Larkin and Yu. N. Ovchinnikov, J. Low Temp. Phys. **63**, 317 (1986); B. I. Ivlev and V. I. Mel'nikov, Phys. Lett. A **116**, 427 (1986); S. Linkwitz and H. Grabert, Phys. Rev. B **44**, 11888 (1991); **44**, 11901 (1991).